JOURNAL OF SPACECRAFT AND ROCKETS
Vol. 47, No. 2, March–April 2010

Open-Loop Spinup and Deployment Control of a Tether Sling

Steven G. Tragesser*
University of Colorado, Colorado Springs, Colorado 80933
and
Bahman Gorjidooz†
ITT Corporation, Colorado Springs, Colorado 80949

DOI: 10.2514/1.46857

A tether sling holds tremendous promise as an energy-storage device, permitting space transportation systems that are capable of injecting a large number of payloads with low incremental costs. This paper develops motor and tether deployment controls to go from rest to a desired final tether length and end velocity. Oscillations in the tether deployment angle are minimized to avoid additional tension in the tether. Open-loop control laws are developed for both power-unlimited and power-constrained cases. For unlimited power, the time-optimal mission profile dictates deployment at large angular velocities. The opposite is true when power is constrained: spinup and deployment time are reduced by deploying at very small angular velocities.

Nomenclature

I_{hub}	=	hub inertia, kg m^2
L	=	tether length, m
m	=	payload mass, kg
P	=	electrical power input at the hub, J/s
r	=	hub length, m
T	=	kinetic energy of system (hub, tether, payload), J
α	=	constant acceleration of the hub, rad/s^2
β	=	ratio of the final tether length at which deployment angle is linearly reduced
θ	=	angular position of hub, rad
ϕ	=	angular position of tether with respect to hub, rad

Subscripts

d	=	time or conditions at end of deployment phase
f	=	time or conditions at end of initial spin phase
i	=	time or conditions at end of initial spin phase

I. Introduction

MANY papers in the literature investigate the use of a nonconducting tether to transfer momentum to a payload. In one scenario, the gravity gradient between the tether end bodies (sometimes assisted by the natural librational motion) is used to boost one end body while the other loses orbital energy [1–6]. This concept depends on the transfer of orbital energy from one body to another and generally takes place over short time frames (minutes to hours). This type of momentum transfer is relevant only to orbiting systems. The fundamental concept was recently demonstrated on the Young Engineers Satellite 2 [7].

The tether sling concept explored in this paper uses electrical power to build up momentum over long periods of time (hours to months). The tether rotates around a hub that can be stationed in orbit or on a body with little to no atmosphere, such as our moon. The tether is, in effect, an energy-storage device, harnessing the kinetic energy until it is ready to be directed along a desired orbital injection. Several papers have considered preliminary design requirements and feasibility of the electric-powered sling [8–11]. Puig-Suari et al. [8] and Jokic and Longuski [9] focus on the power requirements of the system to achieve specific orbital transfers. This research assumes that all the power input into the tether sling is converted into useful kinetic energy to compare the system performance when using conventional propellant. Muller [10,11] considers other aspects of the design, such as the tether sag, and possible designs for achieving a tapered profile in the tether mass and strength.

This paper considers the spinup and deployment dynamics of the tether sling with the motivation of 1) further investigating the concept feasibility at a higher engineering fidelity than in [8–11] and 2) providing baseline designs to determine system requirements such as power. Although Puig-Suari et al. [8] and Jokic and Longuski [9] both investigate power requirements, they do so from an energy balance that is shown in this paper to exclude power losses resulting from the deployment dynamics, which may be as large as the power input (effectively doubling the power requirements). There are only two papers that deal with the dynamics of the tether sling [12,13]. Kuchnicki et al. [12] develop a simple dynamic model consisting of a rigid hub and tether and put forth the first development of a tether sling deployment law. Link and Longuski [13] include the first dynamic analysis of a tapered tether. Both of these references assume a fixed angular velocity for the hub during the tether deployment and a constant deployment rate. Since neither of these references analyze the power required to dynamically drive the system (Kuchnicki et al. [12] plot power, but use an energy balance similar to [8,9]), these deployment laws are not optimized with respect to either the maximum power output or the total power output. Therefore, this paper investigates the spinup and deployment control in greater detail. For an unlimited amount of motor power, the minimum-time deployment law is shown to be identical to the law suggested in [12,13]. When considering constraints on power, however, a large energy loss from the tether tension significantly increases the spinup and deployment time (or, alternately, the requirement on electrical power) over the requirements first developed in [8] and shown in [12,13]. A more-power-efficient deployment profile is suggested in this work, dictating deployment at slower spin rates.

II. Unconstrained Power

For both constrained- and unconstrained-power cases, the system is modeled as a point-mass payload, a massless rigid tether, and a

Presented as Paper 245 at the AAS/AIAA Spaceflight Mechanics Meeting, Savannah, GA, 9–12 Feb. 2009; received 24 Aug. 2009; revision received 30 Dec. 2009; accepted for publication 2 Jan. 2010.

*Assistant Professor, Department of Mechanical and Aerospace Engineering; stragesser@eas.uccs.edu. Senior Member AIAA.

†Technical Staff, P.O. Box 39550, 5009 Centennial Boulevard; bahman.gorjidooz@itt.com. Member AIAA.

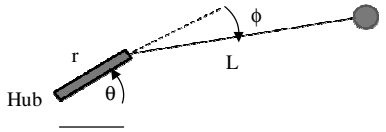

Fig. 1 Tether sling model (top view).

rigid hub. The hub is anchored to an inertially fixed point. Gravity is neglected, and so only planar motion is considered. In reality, gravity causes significant sag in the tether, which may require the sling to be stationed on an area of elevated terrain [11]. If the sling is not stationed along the spin axis of the main body, there may also be significant out-of-plane oscillations, although this issue has not been studied. Aerodynamic drag is also neglected. Therefore, the following analysis is most applicable to a body without an atmosphere, but the general concepts are still relevant to a body with a low atmospheric density (e.g., Mars). As shown in Fig. 1, the displacement of the hub is given by the angle θ, and the displacement of the tether with respect to the radial direction of the tether interface with the hub is given by ϕ. The hub angle is measured positive counterclockwise, and the tether angle is positive clockwise. Nominally, both angles will take on positive values as the system is spun up. The radius of the rigid hub is a constant, r. The variable tether length L will be specified by a deployment law to achieve the desired final length with a minimum of oscillation in ϕ. Oscillation in the tether causes additional undesirable tension in the tether.

A. Equations of Motion

If unlimited power is available to drive a motor on the hub, then any desired motion of the hub can be specified. Therefore, θ can be arbitrarily specified and there is only one generalized coordinate for the system, ϕ, shown in Fig. 1. The kinetic energy for this system is given by

$$T = \tfrac{1}{2}m(r^2\dot{\theta}^2 + \dot{L}^2 + L^2(\dot{\theta}-\dot{\phi})^2) + mrL\dot{\theta}(\dot{\theta}-\dot{\phi})\cos\phi - mr\dot{L}\,\dot{\theta}\sin\phi \tag{1}$$

where m is the mass of the payload.

Using a Lagrangian formulation with no nonconservative forces, the governing equations are obtained from

$$\frac{\mathrm{d}}{\mathrm{d}t}\left(\frac{\partial T}{\partial \dot{\phi}}\right) - \frac{\partial T}{\partial \phi} = 0 \tag{2}$$

Substituting Eq. (1) into Eq. (2) and taking appropriate derivatives gives the single equation of motion:

$$\ddot{\phi} = \frac{1}{L^2}[2L\dot{L}(\dot{\theta}-\dot{\phi}) + rL\ddot{\theta}\cos\phi - rL\dot{\theta}^2\sin\phi] + \ddot{\theta} \tag{3}$$

where $\dot{\theta}$ and $\ddot{\theta}$ are prescribed.

B. Candidate Deployment Strategies

The objective of the sling spinup and tether deployment is to achieve a desired final angular velocity of the hub and final tether length, with no libration in the tether. These terminal end conditions are

$$\dot{\theta}(t_f) = \dot{\theta}_f, \qquad \dot{\phi}(t_f) = 0, \qquad L(t_f) = L_f \tag{4}$$

This end state can be achieved through many different mission profiles. We consider three possible phases for the mission profile: 1) an initial spinup during which the tether is fully retracted ($L = 0$), 2) a deployment phase in which the tether is fully deployed from $L = 0$ to L_f, and 3) a final spinup with the tether length constant ($L = L_f$). Even within this restricted mission profile, there are several possible schemes leading to the desired end state, as shown in Table 1. For the first phase of duration t_i, the initial spinup can terminate in a final angular velocity that is equal to or less than the final desired value $\dot{\theta}_f$. Accelerating the hub to an angular velocity greater than $\dot{\theta}_f$ is also possible, but will not be considered in this paper. For the case in which the initial spinup reaches the final desired angular velocity, the angular velocity remains constant for the deployment phase from time t_i to t_d. Therefore, at the end of the deployment phase, the terminal end conditions from Eq. (4) are satisfied. This is scenario A in Table 1. This is the approach that was developed in [8]. This mission profile is subsequently shown to be time-optimal for unconstrained power. However, in the next section, it is shown that deploying at lower angular velocity is preferable when considering the limited-power case, thereby necessitating investigation of other potential profiles. For the case of an initial spinup to a lower angular velocity, several options exist for the deployment phase. If the hub angular velocity remains constant during deployment, then a final spinup phase (from time t_d to t_f) is necessary. This is scenario B in Table 1. For the remaining two profiles, the hub is accelerated at a constant rate during the deployment phase. In scenario C, the spin rate at the end of the deployment is less than the desired final angular velocity, and so a terminal spinup phase is required. In scenario D, the hub is accelerated to $\dot{\theta}_f$ during the tether deployment, and so no final spin phase is needed. These four profiles represent all possibilities of constant and linearly increasing angular velocity during the deployment and final spinup. These various options for the mission profile are evaluated in Sec. II.D.

C. Open-Loop Control Laws

Throughout the spinup and deployment, the libration of the tether should be kept to a minimum. Oscillation in the tether tends to increase the tether tension, requiring a larger cross-sectional area to accommodate the material stress. Any libration in the tether after the final spinup would need to be damped out to avoid injection errors as the payload is released onto the transfer orbit. To keep tether librations small, the following constraint is enforced when the tether is deploying or fully deployed:

$$\ddot{\phi} = \dot{\phi} = 0 \tag{5}$$

Three different operating conditions are encountered in the four mission scenarios: 1) deploying the tether with a constant hub spin rate, 2) deploying the tether with an accelerating hub, and 3) accelerating the hub with a constant tether length. In this section, the open-loop control laws for the tether deployment rate and tether angle are developed for these three conditions and are referred to as controls I, II, and III, respectively. For control I, the tether deployment law is determined as a function of a constant prescribed deployment angle. For control II, the deployment law is determined for a constant prescribed deployment angle and hub acceleration. For control III, the nominal tether angle is determined for a prescribed hub acceleration.

Table 1 Possible mission scenarios for constant and linearly increasing angular velocities

	Scenario A	Scenario B	Scenario C	Scenario D
Initial spinup ($0 < t < t_i$)	$\dot{\theta}(t_i) = \dot{\theta}_f$	$\dot{\theta}(t_i) < \dot{\theta}_f$	$\dot{\theta}(t_i) < \dot{\theta}_f$	$\dot{\theta}(t_i) < \dot{\theta}_f$
Tether deployment ($t_i < t < t_d$)	$\ddot{\theta} = 0$	$\ddot{\theta} = 0\ \dot{\theta}(t_d) < \dot{\theta}_f$	$\ddot{\theta} = \alpha\ \dot{\theta}(t_d) < \dot{\theta}_f$	$\ddot{\theta} = \alpha\ \dot{\theta}(t_d) = \dot{\theta}_f$
Final spinup ($t_d < t < t_f$)	N/A	$\ddot{\theta} = \alpha$	$\ddot{\theta} = \alpha$	N/A

1. Control I: Tether Deployment with a Constant Hub Spin Rate: $\dot{\phi} = \ddot{\phi} = \ddot{\theta} = 0$

For this case, we wish to find the deployment rate $\dot{L}$ that permits a constant tether angle while the hub angular velocity is constant. From the equation of motion (3),

$$0 = 2L\dot{L}\,\dot{\theta} - rL\dot{\theta}^2 \sin\phi \tag{6}$$

Solving for $\dot{L}$ shows that the tether angle can be kept at an arbitrary nominal constant value by choosing the constant deployment rate:

$$\dot{L} = \frac{r\dot{\theta}}{2}\sin\phi \tag{7}$$

This control law is identical to the deployment law developed by Link and Longuski [13] after simplifying their result for zero tether mass.

2. Control II: Tether Deployment with an Accelerating Hub: $\dot{\phi} = \ddot{\phi} = 0,\ \ddot{\theta} = \alpha$

For this case, we wish to find the deployment rate $\dot{L}$ that permits a constant tether angle while the hub angular acceleration is constant. From Eq. (3),

$$0 = 2\dot{L}\,\dot{\theta} + r\ddot{\theta}\cos\phi - r\dot{\theta}^2 \sin\phi + L\ddot{\theta} \tag{8}$$

Assuming a constant hub acceleration α and rearranging Eq. (8), we find

$$2(\dot{\theta}_0 + \alpha t)\dot{L} + \alpha L = r(\dot{\theta}_0 + \alpha t)^2 \sin\phi - r\alpha\cos\phi \tag{9}$$

This is a nonhomogeneous differential equation with time-varying coefficients of the form

$$\frac{\mathrm{d}L}{\mathrm{d}t} + P(t)L = Q(t) \tag{10}$$

Using the integrating factor

$$\mu(t) = (\dot{\theta}_0 + \alpha t)^{1/2} \tag{11}$$

the differential equation (10) can be expressed as

$$\frac{\mathrm{d}}{\mathrm{d}t}(\mu(t)L(t)) = \mu(t)Q(t) \tag{12}$$

Integrating both sides, dividing by the integrating factor, and applying initial conditions yields the solution for this case:

$$L(t) = \left(r\cos\phi - \frac{r}{5\alpha}\dot{\theta}_0^2 \sin\phi\right)\sqrt{\frac{\dot{\theta}_0}{\dot{\theta}_0 + \alpha t}} + \frac{r}{5\alpha}(\dot{\theta}_0 + \alpha t)^2 \sin\phi - r\cos\phi \tag{13}$$

The tether deployment law is determined by taking the derivative of this solution:

$$\dot{L}(t) = \frac{2r}{5}(\dot{\theta}_0 + \alpha t)\sin\phi - \frac{1}{2}\left(\frac{\alpha}{\dot{\theta}_0}\right) \times \left(r\cos\phi - \frac{r}{5\alpha}\dot{\theta}_0^2 \sin\phi\right)\left(\frac{\dot{\theta}_0}{\dot{\theta}_0 + \alpha t}\right)^{3/2} \tag{14}$$

For the degenerate case of zero hub acceleration, Eq. (14) simplifies to the control I deployment law in Eq. (7).

3. Control III: Hub Acceleration with Constant Tether Length: $\dot{\phi} = \ddot{\phi} = \dot{L} = 0,\ \ddot{\theta} = \alpha$

For this operating condition, the hub is accelerating at a prescribed rate α while the length of the tether remains constant. The equation of motion (3) simplifies to

$$0 = \left(1 + \frac{r}{L_f}\cos\phi\right)\alpha - \frac{r}{L_f}(\alpha t + \dot{\theta}_o)^2 \sin\phi \tag{15}$$

where $\dot{\theta}_o$ is the hub angular velocity at the start of the phase. Solving this equation for the nominal open-loop tether angle yields

$$\phi = \sin^{-1}\left(\frac{c}{\sqrt{a^2 + b^2}}\right) - \tan^{-1}\left(\frac{b}{a}\right) \tag{16}$$

where

$$a = \frac{r}{L_f}(\alpha t + \dot{\theta}_o)^2, \qquad b = -\frac{r}{L_f}\alpha, \qquad c = \alpha \tag{17}$$

For a nonzero acceleration of the hub, the parameter a is time-varying, and therefore ϕ is time-varying. That is, the tether angle cannot be kept constant when the hub is accelerating for a constant length tether. Although this condition violates the assumptions, this pseudoequilibrium tether angle varies slowly with time for small α, and the solution in Eq. (16) is valid for a large range of cases and provides a useful nominal condition.

The solution in Eq. (16) does not exist for large hub accelerations. Setting the argument of the arcsine in Eq. (16) equal to unity at $t = 0$ (which gives the limiting case) admits the following necessary condition on the hub acceleration:

$$\alpha \le \frac{r}{L_f}\sqrt{\frac{1}{1 - r^2/L_f^2}}\dot{\theta}_o^2 \tag{18}$$

Controls I–III are implemented during the appropriate phases of a mission scenario. A mapping of the control laws to the mission scenarios and summary of the control equations is given in Table 2. There is no control identified for the initial spin, since the tether is fully retracted and the system is ideally rigid.

D. Minimum-Time Mission Scenario

Of the four mission profiles shown in Table 1, we determine which requires the minimum time to meet the desired end state in Eq. (4). Since power is unlimited, the hub acceleration is limited only by the tether dynamics; that is, the acceleration is restricted only to keep from inducing librational motion in the tether. This restriction is met via the three open-loop controls developed earlier.

Using the open-loop control, we can analytically calculate the time for each of the mission profiles. For all profiles, the initial spin phase

Table 2 Open-loop control laws for unlimited power

	Scenario A	Scenario B	Scenario C	Scenario D
Initial spin	Rigid-body motion	Rigid-body motion	Rigid-body motion	Rigid-body motion
Tether deployment	Control I, ϕ is an arbitrary constant, and $\dot{L}$ is from Eq. (7)	Control I, ϕ is an arbitrary constant, and $\dot{L}$ is from Eq. (7)	Control II, ϕ is an arbitrary constant, and $\dot{L}$ is from Eq. (14)	Control II, ϕ is an arbitrary constant, and $\dot{L}$ is from Eq. (14)
Final spin	N/A	Control III, $L = L_f$. and ϕ is from Eq. (16)	Control III, $L = L_f$. and ϕ is from Eq. (16)	N/A

is assumed to occur instantly, since the initial configuration is a rigid-body motion with an infinite torque.

1. Scenario A

The total mission time results from the deployment from $L = 0$ to L_f. The deployment rate using control I is maximized by deploying the tether at an angle of $\phi = 90$ deg. The deployment time is obtained by integrating Eq. (7) with a constant hub spin rate of $\dot{\theta}_f$:

$$(t_f)_A = \frac{2L_f}{r\dot{\theta}_f} \tag{19}$$

where $(t_f)_A$ denotes the minimum total mission time for scenario A.

2. Scenario B

This profile consists of a deployment using control I followed by a final spinup. For the spinup control law (control III), the maximum acceleration of the hub (and therefore the minimum spinup time) is the upper bound of Eq. (18). The spinup time for this constant acceleration is obtained from

$$\alpha = \frac{\dot{\theta}_f - \dot{\theta}(t_d)}{t_f - t_d} \tag{20}$$

Substituting the maximum α from Eq. (18) into Eq. (20) gives the time required to increase the hub spin rate from $\dot{\theta}(t_d)$ to $\dot{\theta}_f$:

$$t_f - t_d = \frac{L_f}{r\dot{\theta}(t_d)}\sqrt{1 - \frac{r^2}{L_f^2}}\left(\frac{\dot{\theta}_f}{\dot{\theta}(t_d)} - 1\right) \tag{21}$$

Adding the time for the deployment gives the total mission time for scenario B:

$$(t_f)_B = \frac{L_f}{r\dot{\theta}(t_d)}\sqrt{1 - \frac{r^2}{L_f^2}}\left(\frac{\dot{\theta}_f}{\dot{\theta}(t_d)} - 1\right) + \frac{2L_f}{r\dot{\theta}(t_d)} \tag{22}$$

For $\dot{\theta}(t_d) < \dot{\theta}_f$ this expression is always greater than Eq. (19), and so

$$(t_f)_B > (t_f)_A \tag{23}$$

3. Scenarios C and D

These profiles consist of a deployment using control II followed by a final spinup using control III. A similar expression to Eq. (20) is used to find the time for the hub spinup using a control II deployment:

$$\alpha = \frac{\dot{\theta}(t_d) - \dot{\theta}(t_i)}{t_d - t_i} \tag{24}$$

Substitute this expression into Eq. (13) evaluated at $t = t_d$ to get

$$L_f = \left(r\cos\phi - \frac{r(t_d - t_i)}{5(\dot{\theta}(t_d) - \dot{\theta}(t_i))}\dot{\theta}(t_i)^2\sin\phi\right)\sqrt{\frac{\dot{\theta}(t_i)}{\dot{\theta}(t_d)}} + \frac{r(t_d - t_i)}{5(\dot{\theta}(t_d) - \dot{\theta}(t_i))}\dot{\theta}(t_d)^2\sin\phi - r\cos\phi \tag{25}$$

Solving the preceding equation for the deployment time $t_d - t_i$ gives the total mission time for scenario D:

$$(t_f)_D = \frac{5(\dot{\theta}_f - \dot{\theta}(t_i))}{r\sin\phi(\dot{\theta}_f^2 - \sqrt{[\dot{\theta}(t_i)/\dot{\theta}_f]}\dot{\theta}(t_i)^2)} \times \left(L_f + r\cos\phi\left(1 - \sqrt{\frac{\dot{\theta}(t_i)}{\dot{\theta}_f}}\right)\right) \tag{26}$$

Adding the time for the final spinup yields the total mission time for scenario C:

$$(t_f)_C = \frac{5(\dot{\theta}(t_d) - \dot{\theta}(t_i))}{r\sin\phi(\dot{\theta}(t_d)^2 - \sqrt{[\dot{\theta}(t_i)/\dot{\theta}(t_d)]}\dot{\theta}(t_i)^2)} \times \left(L_f + r\cos\phi\left(1 - \sqrt{\frac{\dot{\theta}(t_i)}{\dot{\theta}(t_d)}}\right)\right) + \frac{L_f}{r\dot{\theta}(t_d)}\sqrt{1 - \frac{r^2}{L_f^2}}\left(\frac{\dot{\theta}_f}{\dot{\theta}(t_d)} - 1\right) \tag{27}$$

The intermediate spin rates and the deployment angle can all be varied to minimize the mission times for these two cases. Using l'Hôpital's rule, the right-hand sides of Eqs. (26) and (27) equal zero as $\dot{\theta}(t_d) \to \infty$ and $\dot{\theta}(t_i) \to \infty$. Since these optimal intermediate spin rates are not feasible, a good practical limit is $\dot{\theta}_f$, for instance, to keep tension levels from exceeding the nominal tension at the final length and spin rate. Evaluating Eqs. (26) and (27) for the constraint $\dot{\theta}(t_i) = \dot{\theta}(t_d) = \dot{\theta}_f$ requires another application of l'Hôpital's rule, yielding

$$(t_f)_C = (t_f)_D = \frac{2L_f}{r\sin\phi\dot{\theta}_f} \tag{28}$$

Therefore, the (constrained) optimal values for scenarios C and D degenerate to scenario A. We conclude that scenario A is the minimum-time spinup and deployment strategy when intermediate spin rates are not allowed to exceed the final spin rate. This is the same strategy as proposed in [8].

The analytic theory is validated with a numerical simulation of the equation of motion (3). The integration is performed using the built-in function `ode45` in MATLAB with default tolerances on the accuracy. The optimal mission strategy is plotted in Fig. 2 for the desired final state:

$$\dot{\theta}(t_f) = 0.05 \text{ rad/s}, \qquad L(t_f) = 20 \text{ km} \tag{29}$$

which gives a payload velocity of 1 km/s. The payload mass is 1000 kg and the length of the hub is 500 m. The tether is deployed at a constant angle of 90 deg, and the tether is deployed at a constant rate of 12.5 m/s. The duration of the mission spinup and deployment, given by Eq. (19), is 1600 s. After the deployment is complete, the equilibrium is along the radial direction, or $\phi = 0$ deg. Since the deployment occurs at a tether angle of 90 deg, a large librational motion about the new equilibrium ensues for $t > 1600$ s. This causes peak tension of 76 kN, which is nearly 50% higher than the nominal value of 51 kN with no libration. The next section develops a modification to the mission profile to help alleviate this problem.

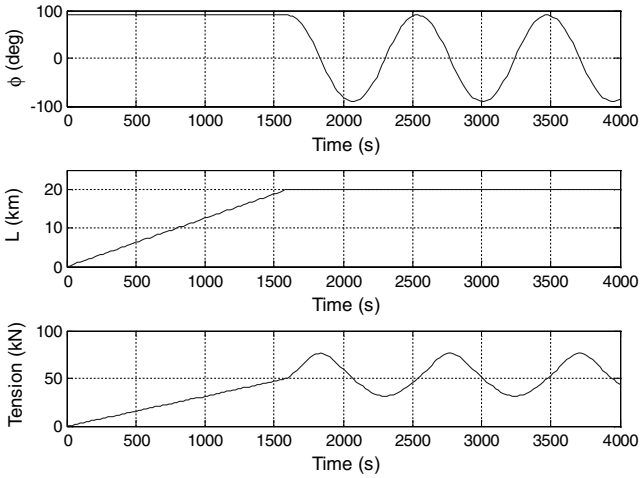

Fig. 2 Scenario A mission results. Total spinup/deployment time is 1600 s. Peak tension is 76 kN.

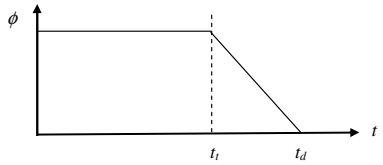

Fig. 3 Modified nominal tether angle to reduce libration.

E. Modified Nominal Open-Loop Tether Angle

Scenario A has a discontinuous nominal value for the tether angle, transitioning from an optimal deployment angle of 90 deg to a equilibrium value of 0 deg at the end of the mission. To smooth this transition, a linear profile for the tether angle is initiated when the tether length is some ratio β of the final length. The point at which this transition begins is denoted as t_t. Figure 3 depicts the modified nominal profile for the tether angle.

The modified nominal tether angle is expressed as

$$\phi(t) = \begin{cases} \frac{\pi}{2} & 0 < t \le t_t \\ \frac{\pi}{2}\left(1 - \frac{t - t_t}{t_d - t_t}\right) & t_t < t < t_d \end{cases} \tag{30}$$

where t_t is obtained from Eq. (22):

$$t_t = \frac{2\beta L_f}{r\dot{\theta}_f} \tag{31}$$

This profile leads to the modified deployment law:

$$\dot{L}(t) = \begin{cases} \frac{r\dot{\theta}_f}{2} & 0 < t \le t_t \\ \frac{r\dot{\theta}_f}{2}\sin\left(\frac{\pi}{2}\left(1 - \frac{t - t_t}{t_d - t_t}\right)\right) & t_t < t < t_d \end{cases} \tag{32}$$

Integrating to obtain a relationship for the deployment time t_d yields

$$t_d = \frac{\pi}{r\dot{\theta}_f}(L_f - \beta L_f) + \frac{2\beta L_f}{r\dot{\theta}_f} \tag{33}$$

The modified nominal tether angle is simulated for $\beta = 0.6$ and is shown in Fig. 4. This gives a transition time of 960 s and increases the deployment time 23% to 1960 s. The libration in the tether angle is significantly reduced from the example in Fig. 2. This reduces the peak value of the tension to 57 kN, or 12% above the nominal value (versus 50% for the constant deployment angle).

III. Constrained Power

A. Equations of Motion

To calculate the power required to drive the system, the dynamics of the hub must be considered. Instead of a prescribed motion, the hub angular displacement θ is a generalized coordinate. The hub inertia is given by I_{hub}. Adding the kinetic energy of the hub to Eq. (1) yields

$$T = \tfrac{1}{2}I_{\text{hub}}\dot{\theta}^2 + \tfrac{1}{2}m(r^2\dot{\theta}^2 + \dot{L}^2 + L^2(\dot{\theta} - \dot{\phi})^2 + 2rL\dot{\theta}(\dot{\theta} - \dot{\phi})\cos\phi - 2r\dot{L}\,\dot{\theta}\sin\phi) \tag{34}$$

A moment τ is applied at the hub by an electric motor. The power input to the motor is assumed to be constant, under the assumption that a minimum-time deployment will use the maximum power available at any given instant. For a given power input, the motor torque is

$$\tau = \frac{P}{\dot{\theta}} \tag{35}$$

where the induced electromagnetic force generated by the angular velocity of the hub is neglected. Applying Lagrange's equations with the generalized force τ gives the equations of motion:

$$\ddot{\phi} - \left(1 + \frac{r}{L}\cos\phi\right)\ddot{\theta} = 2\dot{L}(\dot{\theta} - \dot{\phi}) - \frac{r}{L}\dot{\theta}^2\sin\phi \tag{36a}$$

$$[I_{\text{hub}} + mr^2 + mL^2 + 2mrL\cos\phi]\ddot{\theta} - (mL^2 + mrL)\ddot{\phi} = mr\ddot{L}\sin\phi - 2mL\dot{L}(\dot{\theta} - \dot{\phi}) - 2mr\dot{L}\cos\phi(\dot{\theta} - \dot{\phi}) + mrL\dot{\phi}\sin\phi(\dot{\theta} - \dot{\phi}) + \frac{P}{\dot{\theta}} \tag{36b}$$

where the first equation is identical to the unconstrained-power case.

The same mission phases are considered as for unconstrained power. Each of the three equilibrium configurations is developed subsequently.

B. Open-Loop Control Laws

As in the case of unconstrained power, a minimum libration in the tether angle is desirable. Unfortunately, the constraint

$$\ddot{\phi} = \dot{\phi} = 0 \tag{37}$$

is not achievable for a constant power; that is, both Eqs. (36a) and (36b) cannot be satisfied. However, for large systems with realistic power levels, a pseudoequilibrium tether that is slowly varying can be found using Eq. (37).

1. Control I: Tether Deployment with a Constant Hub Spin Rate: $\dot{\phi} = \ddot{\phi} = \ddot{\theta} = 0$

Solving the equation of motion (36a) yields the same solution for the deployment rate found in Eq. (7). However, the tether deployment angle cannot be chosen arbitrarily; instead, it is dependent on the input power via Eq. (36b). Simplifying this equation for the assumptions of this case and substituting in the tether deployment rate from Eq. (7) yields

$$-mr\dot{\theta}^3(L\sin\phi + r\sin\phi\cos\phi) + P = 0 \tag{38}$$

where L is a time-varying quantity. An analytic solution can be found by assuming a small tether angle, which is valid for large systems with practical input power. Solving Eq. (38) gives

$$\phi = \frac{P}{mr\dot{\theta}^3(L + r)} \tag{39}$$

Assuming a time-linear relationship for $L(t)$ (i.e., constant deployment rate) leads to a solvable time-varying system, but yields inaccurate results. (A constant deployment rate in Eq. (7) is consistent with the assumptions for the pseudoequilibrium, but it is clear from the results in Fig. 5 that a constant deployment rate is not valid.) Better results are obtained by substituting $\phi(L)$ back into Eq. (7) to get a differential equation governing the tether length:

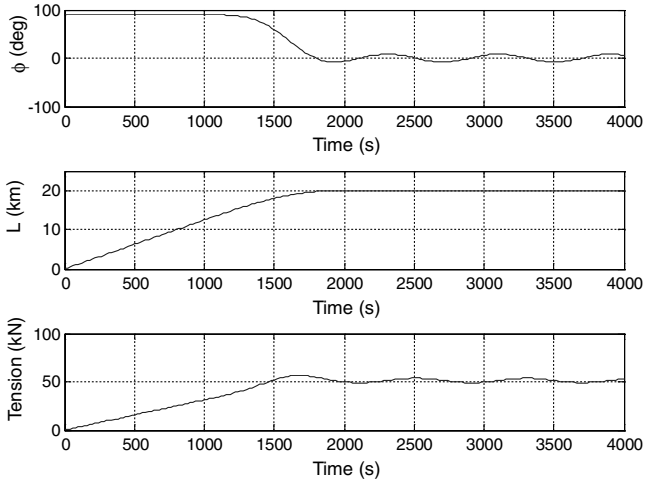

Fig. 4 Scenario A mission results with modified nominal tether angle. Total spinup/deployment time is 1960 s. Peak tension is 57 kN.

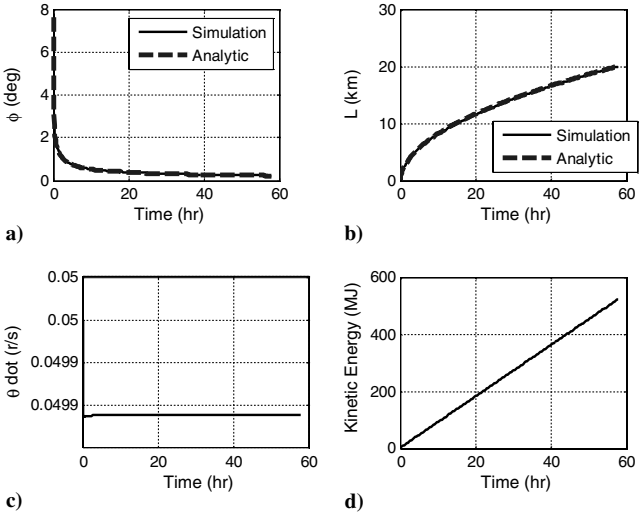

Fig. 5 Scenario A results for 5 kW power. Mission time is 58 h.

$$\dot{L}(L+r) = \frac{P}{2m\dot{\theta}^2} \tag{40}$$

Equation (40) can also be obtained directly from the equation of motion. Integrating leads to a quadratic equation that can be solved to obtain the tether length as a function of time:

$$L(t) = -r + \sqrt{r^2 + \frac{P}{m\dot{\theta}^2}\,t} \tag{41}$$

This expression can be substituted into Eq. (39) to get the tether angle as a function of time:

$$\phi = \frac{P}{mr\dot{\theta}^3}\left(r^2 + \frac{P}{m\dot{\theta}^2}\right)^{-1/2} t^{-1/2} \tag{42}$$

This is a higher-order solution. We have assumed a constant tether angle to get a time-varying expression for the tether angle and substituted that new expression back into the governing equations to solve.

2. Control II: Tether Deployment with an Accelerating Hub: $\dot{\phi} = \ddot{\phi} = 0,\ \ddot{\theta} = \alpha$

Solving the equation of motion (36a) yields the same solution for the deployment length and rate found in Eqs. (13) and (14), respectively. As with the preceding case, the tether angle cannot be chosen arbitrarily, but must satisfy Eq. (36b). For this case, that governing equation is

$$[I_{\text{hub}} + mr^2 + mL^2 + 2mrL\cos\phi](\alpha t + \dot{\theta}_o)\alpha + 2mL\dot{L}(\alpha t + \dot{\theta}_o)^2 + 2mr\dot{L}\cos\phi(\alpha t + \dot{\theta}_o)^2 - P = 0 \tag{43}$$

Because the explicit time dependence of this equation and the more complex form of the tether deployment law, an analytic solution to the tether angle is not easily found. The nominal tether angle can be arrived at via numerical integration.

3. Control III: Hub Acceleration with a Constant Tether Length: $\dot{\phi} = \ddot{\phi} = \dot{L} = 0$

Solving the equation of motion (36a) yields the same solution for the tether angle found in Eq. (16). However, for constant power, a constant hub acceleration is not possible for this case. The hub motion can be solved by simplifying Eq. (36b) for the given assumptions to get

$$I\ddot{\theta}\,\dot{\theta} = P \tag{44}$$

where

$$I = I_{\text{hub}} + m(r^2 + L^2 + 2rL\cos\phi) \tag{45}$$

Integration yields

$$\dot{\theta}(t) = \sqrt{\frac{2Pt}{I} + \dot{\theta}_0^2} \tag{46}$$

Controls I–III are implemented during the appropriate phases of a mission scenario. A mapping of the control laws to the mission scenarios and summary of the control equations are given in Table 3. There is no control identified for the initial spin, since the tether is fully retracted and the system is ideally rigid.

C. Minimum-Time Mission Scenario

The numerical solution for the tether deployment angle using control II precludes an analytic determination of the mission time for scenarios C and D, and so we will limit the minimum-time analysis to the scenarios A and B mission approaches.

1. Scenario A

Since the majority of the energy for a practical system is input during the deployment phase of this mission, the time required to initially spin up the undeployed system to the final desired angular velocity is neglected. The time for the control I deployment is easily obtained by evaluating Eq. (41) at the final time to get

$$(t_f)_A = \frac{m\dot{\theta}_f^2}{P}(L_f + 2L_f r) \approx \frac{m(L_f\dot{\theta}_f)^2}{P} = \frac{2T_f}{P} \tag{47}$$

where T_f denotes the final kinetic energy of the system, and the final equality assumes that the tether angle is small. Rearranging shows that $Pt_f = 2T_f$, or the total energy input into the system, is twice the final kinetic energy. The loss of energy can be explained by considering the negative work done by the tether tension acting opposite the deployment displacement. From Newton's second law, the tension is

$$T = m(r\ddot{\theta}\sin\phi + r\dot{\theta}^2\cos\phi + L(\dot{\theta} - \dot{\phi})^2 - \ddot{L}) \tag{48}$$

Again assuming small tether angles and hub acceleration, then the third term on the right-hand side of the tension expression dominates. The work done by the tension force is approximately

$$W = \int \bar{T}\cdot\bar{v}\,\mathrm{d}t \approx \int mL\dot{\theta}^2\dot{L}\,\mathrm{d}t \tag{49}$$

Substituting the tether length from Eq. (41) and its derivative into Eq. (49) and integrating over the deployment yields

$$W \approx -\tfrac{1}{2}P(t_f - t_i) \tag{50}$$

Table 3 Open-loop control laws for constrained power

	Scenario A	Scenario B	Scenario C	Scenario D
Initial spin	Rigid-body motion	Rigid-body motion	Rigid-body motion	Rigid-body motion
Tether deployment	Control I, ϕ is from Eq. (42), and $\dot{L}$ is from Eq. (41)	Control I, ϕ is from Eq. (42), and $\dot{L}$ is from Eq. (41)	Control II, ϕ is from Eq. (43), and $\dot{L}$ is from Eq. (41)	Control II, ϕ is from Eq. (43), and $\dot{L}$ is from Eq. (41)
Final spin	N/A	Control III, $L = L_f$. and ϕ is from Eq. (16)	Control III, $L = L_f$. and ϕ is from Eq. (16)	N/A

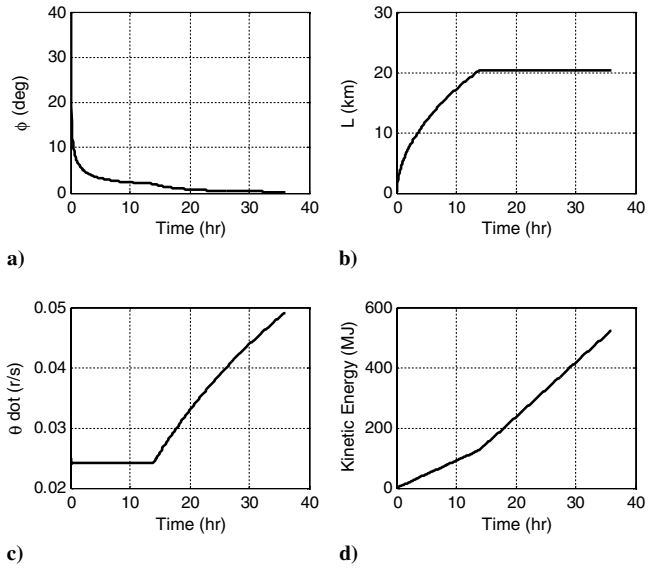

Fig. 6 Scenario B results for 5 kW power. Mission time is 36 h.

So the work from the tension force during the deployment is equal to half of the energy input into the system from the motor. Some of the negative work done by the tension in the tether could be recovered, for example, by running a generator. However, there will always be losses in such a system.

The simulation results for scenario A are shown in Fig. 5 for the same system values as for the unconstrained case, with $I_{\text{hub}} = 2.5 \times 10^8$ kg · m^2 and $P = 5$ kW. The simple deployment law from Eq. (7) governs the tether length in the simulation. The numerical results are accurately represented by the analytic theory in Eq. (41). The maximum deviation for the data in Fig. 5b is 80 m, which represents a maximum percent error of 8%. The tether angle is initialized according to Eq. (42), but the tether angle is not controlled during the simulation. The tether angle ϕ from Eq. (42) also closely matches the simulation results in Fig. 5a. The maximum deviation is 0.2 deg and the maximum percent error is 5%. The librational motion is well-behaved, and no significant oscillation is excited during the deployment, even with no damping or control in the system. Consistent with the assumptions for this deployment, the hub angular velocity is nearly constant, as shown in Fig. 5c. The maximum variation in this parameter is 1.1×10^{-4} rad/s (0.2% error). The kinetic energy increases in a nearly linear fashion to the final desired value of 520 MJ. Calculating the input energy over the duration of the deployment yields

$$E_{\text{input}} = Pt_f = 5 \text{ kW}(58 \text{ h}) = 1040 \text{ MJ} \tag{51}$$

As analytically determined earlier, the input energy is twice the final kinetic energy. From this analysis, we find spinup times that are potentially double those computed in [3,8].

2. *Scenario B*

To get the mission duration for this profile, the time for the final spinup must be determined. Evaluating Eq. (46) at the final time and assuming a small tether angle, the time for this phase is

$$t_f - t_d = \frac{1}{2}\frac{mL_f^2(\dot{\theta}_f^2 - \dot{\theta}(t_i)^2)}{P} \tag{52}$$

Adding the deployment time from Eq. (47) yields a total mission time of

$$(t_f)_B = \frac{1}{2}\frac{mL_f^2(\dot{\theta}_f^2 + \dot{\theta}(t_i)^2)}{P} \tag{53}$$

The mission time is minimized by letting the initial angular velocity (before deployment) go to zero:

$$(t_f)_B = \frac{1}{2}\frac{mL_f^2\dot{\theta}_f^2}{P} \tag{54}$$

This provides a mission time that is exactly half the result for scenario A. Therefore, a scenario B mission approach is optimal when power is constrained. This also yields an equal energy balance between the input energy and the final kinetic energy. That is, there are no energy losses during the mission. The mission times in [3,8] were based upon this energy balance. However, the deployment mechanics rely upon the angular velocity of the hub, and so this is not a realizable scenario. Actual deployment times must be somewhat larger than the result in Eq. (54). Determining the lowest possible hub spin rate during deployment would require a higher-fidelity model, including tether flexibility and elasticity, as well as out-of-plane motion to account for tether sag if the sling is stationed on a large body. This is beyond the scope of this paper.

An example demonstrating the increased efficiency of scenario B is shown in Fig. 6. The hub is initially accelerated to half of the final desired angular velocity, or 0.025 rad/s. The deployment to 20 km requires 14 h for the reduced spin rate. The system is then accelerated with a constant tether length to the final velocity over a period of 22 h. During this time, no energy is lost due to tension in the tether, because there is no displacement of the end mass along the radial direction. The power input from the motor is 400 MJ (5 kW × 22 h), which is equal to the change in kinetic energy during this phase in Fig. 6d. The total mission time of 36 h represents a 38% from scenario A.

IV. Conclusions

Several deployment strategies for a tether sling have been analyzed. If unlimited power is available, the minimum-time scenario implies an initial spinup to the final desired angular velocity followed by deployment of the tether with a constant angular velocity. The optimal strategy is reversed when power constraints are considered. Energy losses from tether braking are shown to waste up to half of the input power from the motor. The system dynamics dictate deployment at the slowest spin rate possible, with the main bulk of the energy added to the system after the tether is fully deployed. These mission profiles provide a baseline for assessment of feasibility and system requirements for the tether sling concept.

References

[1] Carroll, J. A., "Tether Applications in Space Transportation," *Acta Astronautica*, Vol. 13, No. 4, 1986, pp. 165–174. doi:10.1016/0094-5765(86)90061-5

[2] Cosmo, M. L., and Lorenzini, E. C., Tethers in Space Handbook, NASA Marshall Space Flight Center, Rept. NAG8-1160, Huntsville, AL, 1997.

[3] Hoyt, R. P., "Cislunar Tether Transport System ," *Journal of Spacecraft and Rockets*, Vol. 37, No. 2, 2000, pp. 177–186. doi:10.2514/2.3564

[4] Hoyt, R. P., "Momentum-Exchange/Electrodynamic-Reboost Tether Facility for Deployment of Microsatellites to GEO and the Moon," *AIP Conference Proceedings*, Vol. 552, American Inst. of Physics, Melville, NY, 2001, pp. 508–513.

[5] Lanoix, E. L., and Misra, A. K., "Near-Earth Asteroid Missions Using Tether Sling Shot Assist," *Journal of Spacecraft and Rockets*, Vol. 37, No. 4, 2000, pp. 475–480. doi:10.2514/2.3588

[6] French, D. B., and Mazzoleni, A. P., "Asteroid Diversion Using a Long Tether and Ballast," *Journal of Spacecraft and Rockets*, Vol. 46, No. 3, 2009, pp. 645–66.

[7] Kruijff, M., van der Heide, E., Ockels, W. J., and Gill, E., "First Mission Results of the YES2 Tether Space Mail Experiment," American Astronautical Society Paper 08-7385, Aug. 2008.

[8] Puig-Suari, J., Longuski, J. M., and Tragesser, S. G., "A Tether Sling for Lunar and Interplanetary Exploration," *Acta Astronautica*, Vol 36, No 6, 1995, pp. 291–295. doi:10.1016/0094-5765(95)00110-7

[9] Jokic, M. D., and Longuski, J. M., "Design of Tether Sling for Human Transportation Systems Between Earth and Mars," *Journal of Spacecraft and Rockets*, Vol. 41, No. 6, 2004, pp. 1010–1015. doi:10.2514/1.2413

[10] Muller, R. M., "The Slinger—An In-Orbit Booster Facility," AIAA Paper 86-2175, New York, 1986.

[11] Muller, R. M., "The Lunar Slingshot—An Electrically Powered Launcher," *Advances in the Astronautical Sciences*, Vol. 130, No. 1, 2008, pp. 131–8.

[12] Kuchnicki, S. N., Tragesser, S. G., and Longuski, J. M., "Dynamics of a Tether Sling," *Advances in the Astronautical Sciences*, Vol. 97, No. 1, 1997, pp. 91–108.

[13] Link, D. A., and Longuski, J. M., "Dynamics of a Tether Sling System," AIAA Paper 2008-7381, Reston, VA, 2008.

D. Spencer
Associate Editor